

This article was downloaded by:

On: 29 January 2011

Access details: *Access Details: Free Access*

Publisher *Taylor & Francis*

Informa Ltd Registered in England and Wales Registered Number: 1072954 Registered office: Mortimer House, 37-41 Mortimer Street, London W1T 3JH, UK



Supramolecular Chemistry

Publication details, including instructions for authors and subscription information:

<http://www.informaworld.com/smpp/title~content=t713649759>

Chromogenic azole diazothiacrown ethers

Jolanta Szczygelska-Tao^a; Marina S. Fonari^a; Jan F. Biernat^a

^a Gdańsk University of Technology, Gdańsk, Poland

To cite this Article Szczygelska-Tao, Jolanta , Fonari, Marina S. and Biernat, Jan F.(2008) 'Chromogenic azole diazothiacrown ethers', *Supramolecular Chemistry*, 20: 7, 651 – 658

To link to this Article: DOI: 10.1080/10610270701666000

URL: <http://dx.doi.org/10.1080/10610270701666000>

PLEASE SCROLL DOWN FOR ARTICLE

Full terms and conditions of use: <http://www.informaworld.com/terms-and-conditions-of-access.pdf>

This article may be used for research, teaching and private study purposes. Any substantial or systematic reproduction, re-distribution, re-selling, loan or sub-licensing, systematic supply or distribution in any form to anyone is expressly forbidden.

The publisher does not give any warranty express or implied or make any representation that the contents will be complete or accurate or up to date. The accuracy of any instructions, formulae and drug doses should be independently verified with primary sources. The publisher shall not be liable for any loss, actions, claims, proceedings, demand or costs or damages whatsoever or howsoever caused arising directly or indirectly in connection with or arising out of the use of this material.

Chromogenic azole diazothiacrown ethers

Jolanta Szczygelska-Tao*, Marina S. Fonari¹ and Jan F. Biernat

Gdańsk University of Technology, Gdańsk, Poland

Azocrown ethers with sulphur atoms and pyrrole or imidazole residue as a part of macrocycle have been synthesised. Their metal complexation abilities in acetonitrile were studied using UV–vis spectrophotometry. The largest spectral changes were observed for both pyrrole- and imidazole-azothiacrown ethers on complexation with Pb^{2+} , Cu^{2+} , Zn^{2+} , Ni^{2+} , Co^{2+} and Ag^+ ions. In the case of alkali and alkaline earth metal ions no spectral changes were found. Preliminary studies of ion-selective membrane electrodes with synthesised ionophores are presented. In the measurement for transition/heavy metal cations, only copper and lead give high responses. X-ray structure of 18-membered pyrrole azothiacrown ether is described.

Keywords: chromoionophores; azole azothiacrowns; X-ray structure; complexation; ion-selective electrodes

Introduction

Despite the fact that cation recognition has been extensively studied over a century, reagents selectively binding particular cations are still in great demand. An interesting group of such reagents are chromoionophores, which are macrocyclic compounds changing colour upon interaction with metal cations (1). The diameter of the macrocyclic cavity and the kind of donor atoms in the macroring differentiate complexed species according their size and/or other specific properties. This type of chromoionophores were developed mainly with respect to alkali and alkaline earth metal cations. However, design and synthesis of reagents specifically recognising heavy/transition metal ions are still not as extensive as desired. Within azochromoionophores (2) a special attention was paid to macrocyclic compounds with inherent $-\text{N}=\text{N}-$ unit. Previously, we showed that 18- and 21-membered chromogenic derivatives of *p*-alkylphenol with an inherent azo unit can be used for the detection of small concentration of lithium cations (3). Crown ethers, in which ‘hard’ oxygen atoms of the ether chain are replaced with ‘soft’ sulphur atoms show complementary properties, i.e. increased affinity towards transition metal ions with discrimination of alkali and alkaline earth ions (1, 4, 5). It was expected that expansion of such compounds by a heterocyclic unit may create chromoionophores manifesting further differentiation of complexation selectivity.

This work presents the synthesis and study of chromogenic azothiacrown reagents (1–7, Scheme 1 with two azo units and pyrrole or imidazole residue as a part of macrocycle [c.f. 6.7]. Considering earlier studies

of the respective oxa-analogues (8–9, Scheme 1) (6, 12), we expected wider variety of complexed ions, especially transition/heavy metal ions.

Results and discussion

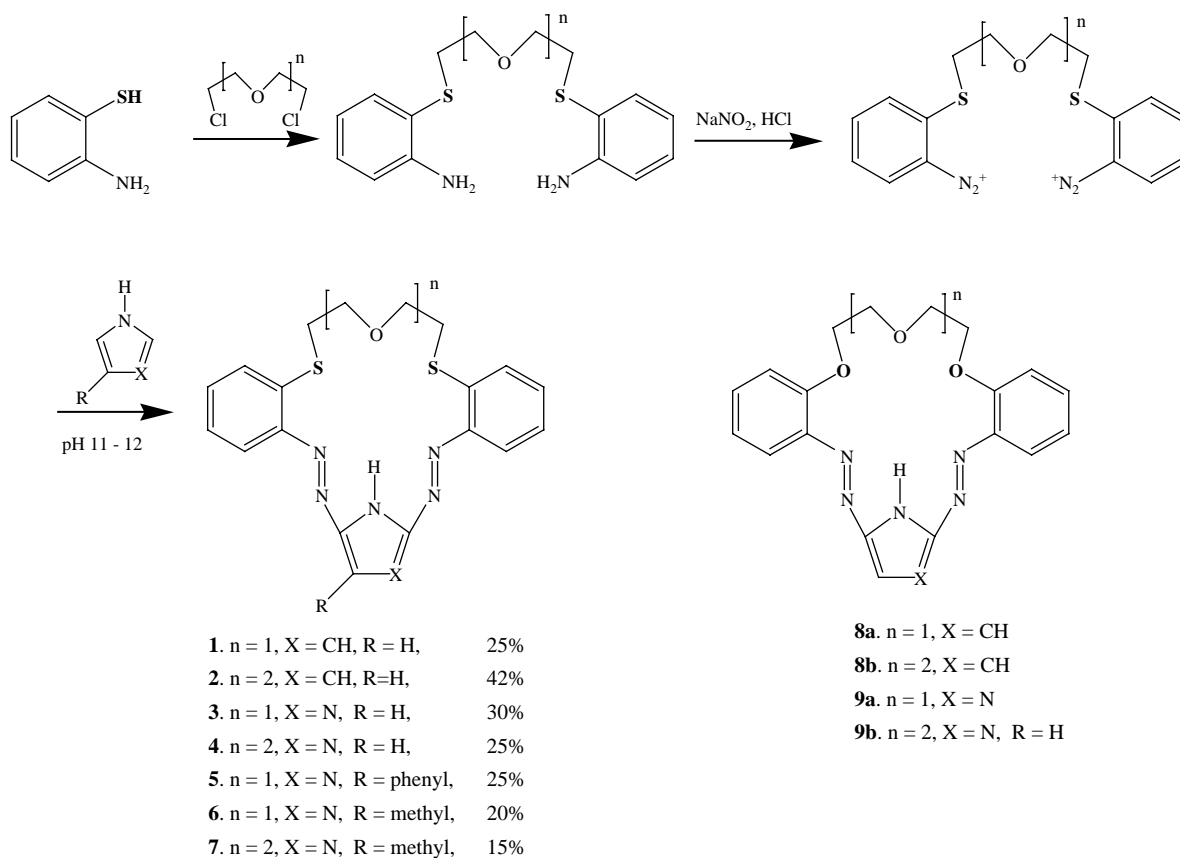
The 18- and 21-membered pyrrole- or imidazole-azothiacrown ethers were obtained in two consecutive reactions (3,7) (Figure 1), i.e. (1) alkylation of 2-aminobenzenethiol with the respective 1,5-dichloro-3-oxapentane or 1,8-dichloro-3,6-dioxaoctane to form diaminodithioethers; and (2) diazotization of the diamine, followed by coupling of the bis-diazonium salts with pyrrole or imidazole with simultaneous macrocyclisation. The coupling reaction was performed under high dilution conditions at $\text{pH} \sim 13$ (NaOH). The products were extracted and pure compounds were isolated by column chromatography. Yield of the obtained compounds 1–7 ranging from 15 to 42% was satisfactory.

The obtained compounds are coloured, crystalline compounds well soluble in organic solvents. Their spectra change in acetonitrile upon addition of acid (HClO_4) or base (Me_4NOH) only at extreme values of $\text{pH}(\text{s})$.

The complexation studies of pyrrole 1, 2 or imidazole 3–7 derivatives were carried out by spectrophotometric titration with metal perchlorates in acetonitrile.

The largest spectral changes were observed for both pyrrole- and imidazole-azothiacrown ethers on complexation with Pb^{2+} , Cu^{2+} , Zn^{2+} , Ni^{2+} , Co^{2+} and Ag^+ ions. In the case of alkali and alkaline earth metal ions no spectral changes were found. This is on the contrary

*Corresponding author. Email: jolas-t@chem.pg.gda.pl



Scheme 1. Synthesis of azole azothiacrown ethers.

to previously described (6) rather high stability constants for Ca^{2+} , Sr^{2+} and Ba^{2+} complexes with 18-membered pyrrole oxa-analogue **8a**. On the other hand, the 21-membered pyrrole analogue **8b** selectively forms complexes with potassium ($\log K_{\text{K}} \sim 4$) and barium ($\log K_{\text{Ba}} = 4.59$).

In the case of pyrrole azothiacrown **1** the most significant spectral changes were found for complexation of copper (Figure 2), lead and silver. These ions were found to be completely complexed within the time scale of the initial spectrophotometric measurement. Complexation is followed by colour change from red to blue.

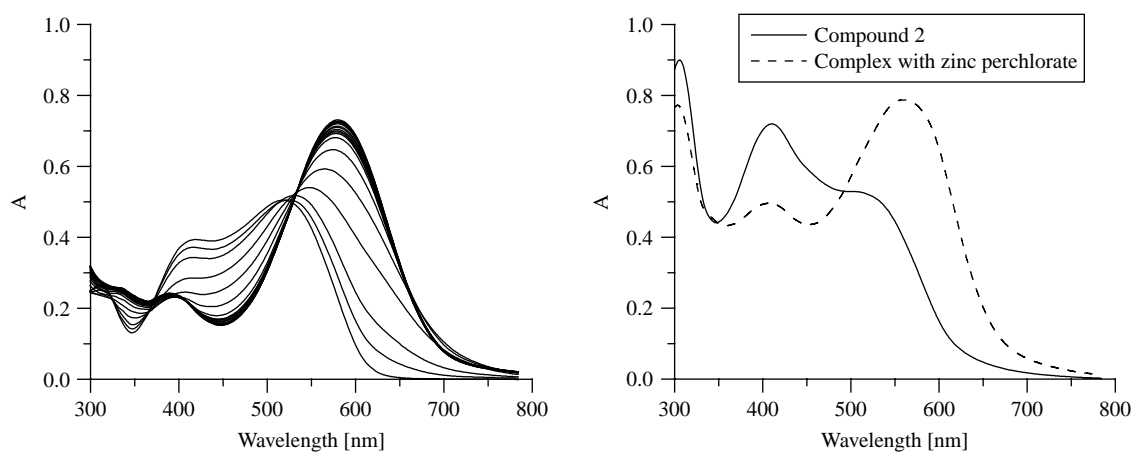


Figure 1. Left: Changes in absorption spectra upon titration of 18-membered pyrrole derivative **1** ($c = 3.66 \times 10^{-5} \text{ M}$) with $\text{Cu}(\text{ClO}_4)_2$ ($c = 1.31 \times 10^{-3} \text{ M}$). Right: limiting spectrum for 21-membered pyrrole derivative **2** ($c = 1.39 \times 10^{-3} \text{ M}$) upon titration with $\text{Zn}(\text{ClO}_4)_2$ ($c = 10^{-3} \text{ M}$).

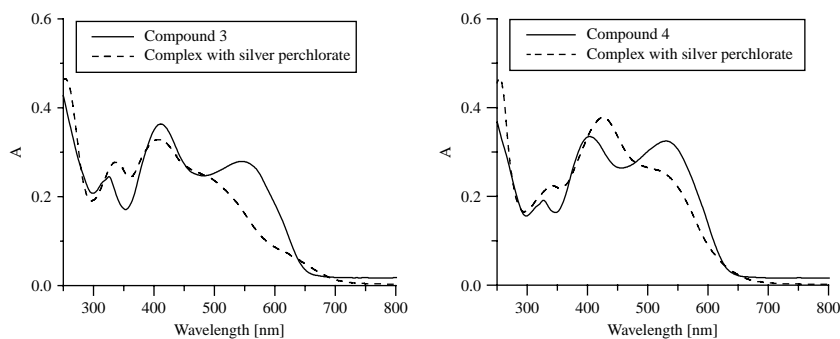


Figure 2. Left: Limiting spectrum for 18-membered imidazole derivative **3** ($c = 2.8 \times 10^{-5}$ M) upon titration with AgClO_4 ($c = 1.1 \times 10^{-3}$ M); right: limiting spectrum for 21-membered imidazole derivative **4** ($c = 2.6 \times 10^{-5}$ M) upon titration with AgClO_4 ($c = 1.1 \times 10^{-3}$ M).

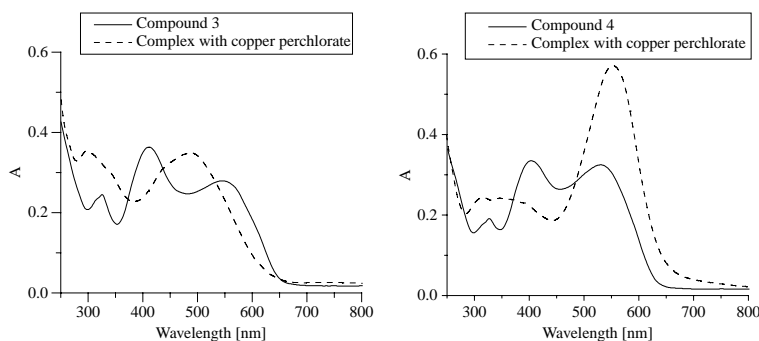


Figure 3. Left: Limiting spectrum of 18-membered imidazole derivative **3** ($c = 2.8 \times 10^{-5}$ M) upon titration with $\text{Cu}(\text{ClO}_4)_2$ ($c = 1.05 \times 10^{-3}$ M); right: limiting spectrum for 21-membered imidazole derivative **4** ($c = 2.6 \times 10^{-5}$ M) upon titration with $\text{Cu}(\text{ClO}_4)_2$ ($c = 1.05 \times 10^{-3}$ M).

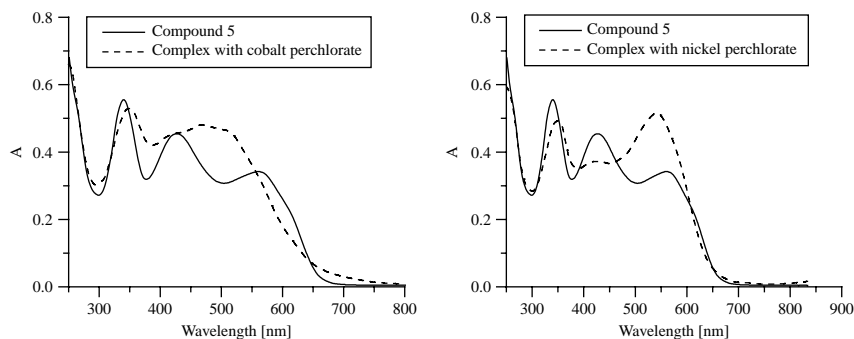


Figure 4. Left: Limiting spectrum of 18-membered phenylimidazole derivative **5** ($c = 9.26 \times 10^{-5}$ M) upon titration with $\text{Co}(\text{ClO}_4)_2$ ($c = 1.21 \times 10^{-3}$ M); right: limiting spectrum for 18-membered phenylimidazole derivative **5** ($c = 9.26 \times 10^{-5}$ M) upon titration with $\text{Ni}(\text{ClO}_4)_2$ ($c = 1.18 \times 10^{-3}$ M).

Upon copper complexation in the spectrum of **1** (Figure 2, left) the intensity of absorption band at 410 nm decreases whereas the band at 520 nm undergoes bathochromic shift (570 nm) with simultaneous increase of intensity. Similar spectral changes were observed for compound **1** on lead and silver ions complexation. Stability constants for copper, lead and silver complexes were determined using the Goldenberg method (8).

For silver the complex stoichiometry is 1:1 whereas copper and lead form 2:1 (L:M) complexes. Nickel, cobalt and zinc cations also form complexes with azothiacrown ether **1**; however the equilibration process is slow, which is in agreement with more inert nature of these ions. The data collected even after 12 h of reaction do not allow to calculate the respective stability constants (Table 1).

Table 1. Stability constants and stoichiometry (L:M) for pyrrole **1,2** and imidazole **3–7** azothiacrown ether complexes of transition metal cations in acetonitrile at room temperature ($20^{\circ}\text{C} \pm 1$).

Compound	Log K_{Me}					
	Pb ²⁺ (2:1)	Cu ²⁺ (2:1)	Zn ²⁺ (1:1)	Ag ⁺ (1:1)	Ni ²⁺ (2:1)	Co ²⁺ (2:1)
1	9.8	12.0	*	11.9	*	*
2	11.1	11.7	10.8	9.6	*	*
3	10.6	11.5	8.8	10.3	9.8	9.5
4	8.5	10.3	9.8	11.7	8.6	7.9
5	9.8	8.8	10.7	9.9	11.7	10.6
6	*	10.4	9.5	10.2	10.6	8.4
7	8.9	9.6	*	11.4	9.9	*

*Changes in spectra do not allow to determine the stability constants.

In the case of compound **2**, spectral (and colour) changes upon complexation are similar. Zinc forms 1:1 complex with stability constant equal to 10.79. A hypochromic effect was found for the band at 410 nm, whereas the band at 520 nm increases with bathochromic shift (60 nm) (Figure 2, right). Stability constants for Pb²⁺, Cu²⁺ and Ag⁺ complexes with **2** are listed in Table 1. Analogously to compound **1**, ionophore **2** reacts too slowly with nickel and cobalt ions to determine of log K .

The 18-membered imidazole-azocrown ether **9a** selectively forms complexes with Na⁺, Mg²⁺, Ca²⁺, Sr²⁺ and Ba²⁺ in a selective manner (6). Compound **3**, the thia-analogue of **9a** is spectroscopically insensitive towards alkali and alkaline earth cations.

The 18- and 21-membered azothiacrowns **3** and **4** react relatively fast with all studied cations; the stability constants are collected in Table 1. Figure 3 presents the results of titration of compounds **3** and **4** with silver. Complex formation is accompanied by colour change from red to yellow. For compound **3** the band at 410 nm shows bathochromic shift upon titration with copper salt, whereas the band at 550 nm practically disappears (Figure 4, left). For titration of **4** with copper ions hyperchromic effect is very characteristic (Figure 4, right). Initially red solution changes colour to pink in case of **3** and to blue for compound **4**.

Compound **5**, the azothiacrown with phenylimidazole residue shows interesting colour changes from red to blue

upon titration with nickel salt, whereas cobalt ions cause change to pink. The limiting spectra are shown in Figure 5; cf. also stability constants for other cations, Table 1.

Compound **6** reacts unexpectedly slowly with lead cations, whereas **7** reacts slowly with zinc and cobalt ions. Both compounds form the most stable complexes with copper, silver and nickel ions (Table 1).

Studies of cadmium(II) complexation were not performed due to solubility restrictions.

Ion-selective membrane electrodes

It was proved that membrane electrodes containing pyrrole derivatives **8** are potassium selective, whereas the respective imidazole derivative **9** shows good selectivity for sodium over potassium with $\log K_{\text{Na,K}}^{\text{pot}} = -1.77$ (6). With reference to this investigation, potentiometric studies of ion-selective electrodes with membranes doped with azothiacrown ethers **1–7** were performed under identical conditions.

Electrodes were characterised using neutral salt solutions. Preliminary studies for hydrogen ion were also performed, but the electrode responses in the concentration range 10^{-7} – 10^{-4} mol dm⁻³ was negligible. Potentiometric selectivity coefficients given as $\log K_{\text{Cd,X}}^{\text{pot}}$ (X, interfering cation) were obtained using separate solution method (9) for mono- and divalent cations (Table 2). Electrodes containing pyrrole **1** or imidazole **3**

Table 2. Selectivity coefficients $\log K_{\text{Cd,X}}^{\text{pot}}$ for membrane electrodes containing pyrrole **1,2** and imidazole **3–7** derivatives.

Compound	S [mV] for Cd	$\log K_{\text{Cd,X}}^{\text{pot}}$						
		K ⁺	Na ⁺	Ca ²⁺	Cu ²⁺	Ni ²⁺	Co ²⁺	Pb ²⁺
1	28	8.13	8.55	–	3.63	–0.02	0.21	5.35
2	28	2.39	1.35	–4.90	6.50	–3.21	–3.19	4.25
3	27	9.14	10.15	0.34	8.37	2.85	3.51	6.45
4	29	–0.24	1.22	–	5.89	–2.17	–1.68	3.62
5	28	– 1.01	2.40	–6.57	1.18	–5.49	–5.08	–2.45
6	29	1.22	1.08	–3.66	2.22	0.12	1.36	3.66
7	27	2.25	0.55	–1.25	3.08	1.35	2.07	4.55
Blank	29	5.90	2.62	–0.45	1.63	1.26	2.25	1.12

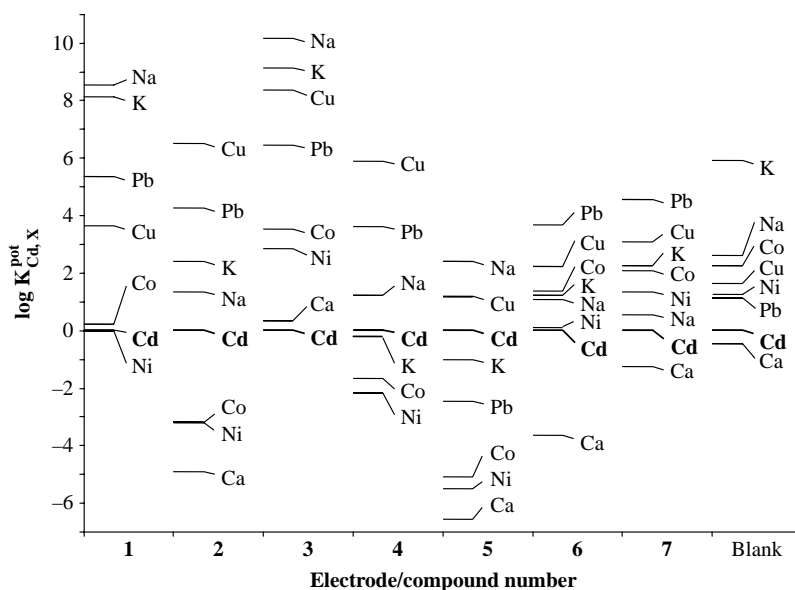


Figure 5. $\log K_{Cd,X}^{pot}$ values of membrane electrodes.

derivatives show surprisingly high potassium and sodium response but the sodium over potassium selectivity is low. The selectivity coefficients $\log K_{Cd,X}^{pot}$ in relation to cadmium equal 8.13 and 9.14 for potassium, and 8.55 and 10.15 for sodium, respectively. On the other hand, the responses for transition metal cations are unexpectedly low. The interesting results were obtained for compound **5**. The difference between the selectivity coefficients for sodium and potassium is high and equals about 3.40. It can suggest that those cations can be differentiated in solution, but copper and cadmium ions interfere. In the measurement for transition/heavy metal cations, only copper and lead give relatively high responses (10, 11). The slopes for cadmium ions are given in Table 1; the slopes for other cations are nernstian.

X-ray structure of **1**

The X-ray structure of compound **1** with displacement ellipsoids and atomic numbering scheme is shown in Figure 6. The details of structure solution and refinement are given in Table 3. Compound **1** crystallises in space group *Pbca*. The 18-membered macrocycle consists of a thioxoethylene chain and rigid cyclic moieties (two phenyl and one pyrrole rings) joined by two azo groups. Both azo groups in the molecule adopt *E*-form with *trans*-arrangement of the phenyl- and pyrrole fragments. In this part of the macrocycle, the aromatic units approach coplanarity; the dihedral angles between the planes through phenyl(1)(C5 > C10)–pyrrole(N3,C11 > C14), pyrrole(N3,C11 > C14)–phenyl(2)(C15 > C20) and phenyl(1)–phenyl(2) rings are equal to 6.3, 6.5 and 6.8°,

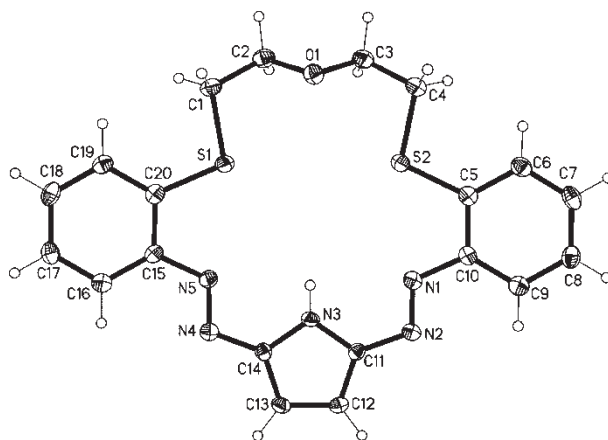


Figure 6. ORTEP view for compound **1** with atomic numbering scheme.

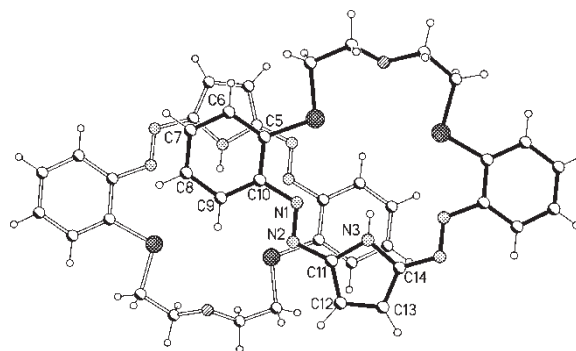


Figure 7. The offset overlapping of centre-of-inversion related macrocycles in the crystal.

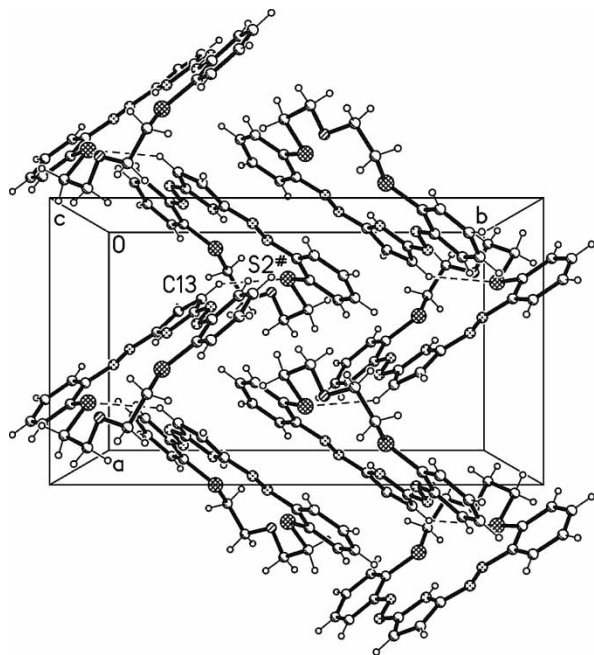


Figure 8. Fragment of the crystal packing for molecules **1**. The CH...S interaction is shown by dotted line.

correspondingly. Because of the constraints imposed by the extended rigid segment of the molecule, the conjugated system comprising six carbon and five nitrogen atoms, C20/C15/N5/N4/C14/N3/C11/N2/N1/C10/C5, acquires

practically flat a conformation in which the atoms lie within $\pm 0.0423 \text{ \AA}$ of the mean plane, which they define (Figure 6).

The shape of the macrocyclic skeleton, even though the pronounced flattening, closely mimics the crown-like shape of 18-crown-6 molecule (the heteroatoms of the $\text{N}_3\text{S}_2\text{O}$ set being oriented in an *endo*-dentate mode and coplanar within $\pm 0.0404 \text{ \AA}$, whereas for 18-crown-6 the corresponding value is $\pm 0.24 \text{ \AA}$). Along the 18-membered heterocyclic framework two successive bonds in the *anti*-conformation alternate with one bond in *gauche*- (C–C bond) or *cis*- (C–C or N–C bonds) conformations. All C–S bonds adopt *anti*-conformation. It is different from an usual *exo*-orientation of sulphur atoms in saturated macrocycles and *gauche*-conformation typical for C–S linkages (12).

In the crystal, two molecules related by the inversion centre form the centrosymmetric dimer sustained by the offset π – π staking interacting between the partially overlapping planar fragments combining one phenyl and pyrrole rings (Figure 7). The interplanar distance equals to 3.25 \AA which corresponds to π – π stacking interactions between the aromatic moieties (13).

These dimers are arranged in a herringbone mode (Figure 8) with the dihedral angle between the planes through their $\text{N}_3\text{S}_2\text{O}$ set of heteroatoms equal to 80.3° . The neighbouring molecules being in a T-shape arrangement and related by the two-fold screw axis are coupled by the shortest in the structure C13...S2($-0.5 + x, 0.5 - y, 1 - z$) contact equal to 3.607 \AA (along *a* axis).

Table 3. Crystal data and structure refinement details for compound **1**.

Empirical formula	$\text{C}_{20}\text{H}_{19}\text{N}_5\text{OS}_2$
Formula weight	409.52
Temperature (K)	100(2)
Wavelength (\AA)	0.71073
Crystal system, space group	Orthorhombic, <i>Pbca</i>
Unit cell dimensions	
<i>a</i> (\AA)	9.8153(5)
<i>b</i> (\AA)	16.9047(10)
<i>c</i> (\AA)	23.0042(11)
<i>V</i> (\AA^3)	3817.0(3)
<i>Z</i> , <i>D_x</i> (Mg/m^3)	8, 1.425
μ (mm^{-1})	0.301
<i>F</i> (000)	1712
Crystal size (mm)	$0.70 \times 0.30 \times 0.07$
θ range for data collection, deg.	2.57 to 25.00
Limiting indices	$-11 \leq h \leq 11, -19 \leq k \leq 20, -27 \leq l \leq 27$
Reflections collected/unique	33613/3350 [R(int) = 0.0572]
Refinement method	Full-matrix least-squares on F^2
Data/restraints/parameters	3350/0/257
Goodness-of-fit on F^2	1.054
Final <i>R</i> indices [$I > 2\sigma(I)$]	$R_1 = 0.0409, wR_2 = 0.0830$
<i>R</i> indices (all data)	$R_1 = 0.0669, wR_2 = 0.0920$
Largest diff. peak and hole ($\text{e}^{-\text{\AA}^{-3}}$)	0.250 and -0.246

Experimental

General

All materials and solvents used for syntheses were of analytical grade. Silica gel (0.035–0.070 mm, Fluka) was used for column chromatography. ^1H NMR spectra were recorded on a Varian instrument at 500 MHz. IR spectra were recorded on Genesis II (Mattson) apparatus. The purity and identity of crown ethers was established by high-resolution mass spectra carried out on a AMD-604 spectrometer. UV–vis spectra were recorded on a Unicam UV-330 Spectrophotometer. For potentiometric measurements, 654 pH-meter (Metrohm) and OP-08201 Ag/AgCl Radelkis reference electrode was used. The mps ($^{\circ}\text{C}$) are uncorrected.

Syntheses

The syntheses were performed using high dilution technique. Two solutions were prepared.

Solution A: A suspension of the respective bis-amine (2 mmol) (*14*) in 40 ml water was cooled in an ice-bath and acidified with conc. hydrochloric acid (1 ml). The amine was diazotised with sodium nitrite (0.28 g, 4.1 mmol) dissolved in 2 ml of ice-cold water.

Solution B: Pyrrole, imidazole or imidazole derivative (2 mmol) and sodium hydroxide (0.2 g, 5 mmol) were dissolved in water (40 ml) and ethanol (2 ml) mixture.

The above cold solutions *A* and *B* were dropped with the same speed during 30 min. into 800 ml of vigorously stirred water (pH \sim 13, NaOH). The temperature of the aqueous medium was kept at 5°C . Stirring was continued for 1 h at this temperature and then for about 12 h at room temperature. The crude product was extracted with methylene chloride and ethyl acetate. The combined extracts were evaporated to dryness and the azothiacrown ethers were isolated on column chromatography using methylene chloride as the initial eluent and then with a methylene chloride–acetone (10:1) mixture.

Compound 1. Yield 25%, dark red crystals (from ethanol), mp $196\text{--}198^{\circ}\text{C}$. HRMS (EI): 409.10323, $\text{C}_{20}\text{H}_{19}\text{N}_5\text{OS}_2$ requires 409.10310. ^1H NMR 3.33s (4H), 3.95s (4H), 7.18s (2H), 7.30–7.60m (6H), 8.10s (2H), 10.50 (\sim 1H). IR ν_{max} (film): 3435; 2931; 2870; 1586; 1485; 1446; 1374; 1276; 1119; 1029; 751 cm^{-1} .

Compound 2. Yield 42%, dark red solid, mp $174\text{--}176^{\circ}\text{C}$ HRMS (EI): 453.12944, $\text{C}_{22}\text{H}_{23}\text{N}_5\text{O}_2\text{S}_2$ requires 453.12932. ^1H NMR 3.33s (4H), 3.72s (4H), 3.93s (4H), 7.22s (2H), 7.25–7.75m (6H), 8.10s (2H), 10.50 (\sim 1H). IR ν_{max} (film): 3589; 3496; 3010; 2918; 1587; 1486; 1450; 1388; 1277; 1249; 1161; 1110; 1056; 950; 843; 752; 667; 613 cm^{-1} .

Compound 3. Yield 30%, deep red solid mp $158\text{--}160^{\circ}\text{C}$ HRMS (EI): 410.09673, $\text{C}_{19}\text{H}_{18}\text{N}_6\text{OS}_2$ requires 410.09835. ^1H NMR 3.33s (4H), 3.95s (4H), 7.18–7.28m (2H), 7.33–7.46m (4H), 7.73dd (1H), 7.85dd (1H), 8.6s

(1H), 10.5 (\sim 1H). IR ν_{max} (nujol): 1589; 1540; 1261; 1234; 1159; 1112; 1054; 1019; 940; 754 cm^{-1} .

Compound 4. Yield 25%, red solid, mp $138\text{--}140^{\circ}\text{C}$ HRMS (EI): 454.12486, $\text{C}_{21}\text{H}_{22}\text{N}_6\text{O}_2\text{S}_2$ requires $M = 454.12457$. ^1H NMR 3.31s (4H), 3.74s (4H), 3.91s (4H), 7.20–7.25m (2H), 7.37–7.46m (4H), 7.74d (1H), 7.91d (1H), 8.16s (1H), 10.5 (\sim 1H). IR ν_{max} (nujol): 1589; 1535; 1348; 1300; 1281; 1234; 1159; 1112; 1080; 990; 754 cm^{-1} .

Compound 5. Yield 25%, red solid, mp $192\text{--}194^{\circ}\text{C}$ HRMS (EI): 486.12863, $\text{C}_{25}\text{H}_{22}\text{N}_6\text{OS}_2$ requires 486.12965. ^1H NMR 3.31s (4H), 3.98s (4H), 7.18dd (2H), 7.28–7.33m (2H), 7.37t (1H), 7.44t (2H), 7.52t (2H), 7.81d (1H), 7.92d (1H), 8.52d (2H), 10.5 (\sim 1H). IR ν_{max} (nujol): 1586; 1535; 1318; 1300; 1271; 1224; 1156; 1072; 940; 754; 670; 557 cm^{-1} .

Compound 6. Yield 20%, red solid, mp $174\text{--}176^{\circ}\text{C}$ HRMS (EI): 328.4523, $\text{C}_{20}\text{H}_{20}\text{N}_6\text{OS}_2$ requires 328.4516. ^1H NMR 1.2s (3H), 3.33s (4H), 3.95s (4H), 7.18–7.28m (2H), 7.33–7.46m (4H), 7.73dd (1H), 7.85dd (1H), 8.6s (1H), 10.5 (\sim 1H). IR ν_{max} (film): 3566; 3490; 2910; 1460; 1435; 1368; 1240; 1161; 1110; 1046; 946; 752 cm^{-1} .

Compound 7. Yield 15%, red solid, mp $156\text{--}158^{\circ}\text{C}$ HRMS (EI): 372.5061, $\text{C}_{22}\text{H}_{24}\text{N}_6\text{O}_2\text{S}_2$ requires 372.505. ^1H NMR 1.25s (3H), 3.35s (4H), 3.95s (4H), 7.18–7.28m (2H), 7.33–7.46m (4H), 7.73dd (1H), 7.85dd (1H), 8.5s (1H), 10.4 (\sim 1H). IR ν_{max} (film): 3570; 3488; 1587; 1486; 1450; 1380; 1268; 1254; 1161; 1056; 942; 843; 748; 667 cm^{-1} .

Determination of stability constants

The Stability constants of azole thiacycrown ether complexes with metal cations were determined by spectrophotometric titrations. The spectra were recorded up to a high excess of cation to crown ether and finally the limiting spectra were obtained. The dependence of the absorbance versus metal salt concentration was described well by equation $(A_0 - A)/(A - A_i) = K[M^+]$ (8), where A is absorption of a sample, A_0 and A_i are the values of absorbances at zero and infinite salt concentration, respectively. Data taken at least at three different wavelengths were fitted to the above equation.

Membrane preparation and potentiometric measurements

Preparation of membranes for ion-selective electrodes has been described earlier in details (15). The typical composition of membranes is: ionophore 5 mg, potassium tetrakis(*p*-chlorophenyl)borate 0.5 mg, poly(vinylchloride) 50 mg and *o*-nitrophenyl octyl ether 0.1 ml. The internal electrolyte was 1 mol dm^{-3} potassium chloride solution. The electrodes were soaked in $10^{-2}\text{ mol dm}^{-3}$ KCl solution before measurements. The selectivity coefficients were

determined using the separate solution method (SSM) (16) at 10^{-2} mol dm⁻³ activities of metal cations.

X-ray crystal structure analysis of compound 1

A single crystal of compound **1** was obtained by crystallisation from propan-2-ol. All measurements were performed at 100 K on a Kuma KM4CCD κ -axis diffractometer with graphite-monochromated Mo K α radiation. The crystal was positioned at 65 mm from the KM4CCD camera. A total of 1204 frames were measured at 1.0° intervals with a counting time of 24 s. The data were corrected for Lorentz and polarisation effects. The numerical absorption correction was applied. Data reduction and analysis were carried out with the Kuma Diffraction (Wrocław) programs (17). The structure was solved by direct methods (18) and refined using SHELXL (19). The refinement was based on F^2 for all reflections except those with very negative F^2 . Weighted R factors wR and goodness-of-fit S value are based on F^2 . The $F_0^2 > 2\sigma(F_0^2)$ criterion was used only for calculating R factors and is not relevant to the choice of reflections for the refinement. All hydrogen atoms except the one attached to the pyrrole ring were put in idealised averaged geometrical positions, allowed to ride at the heavy atoms. The H-atom attached to the pyrrole nitrogen was localised on the different Fourier map and refined isotropically.

Supplementary data are deposited with the Cambridge Crystallographic Data Centre as a supplementary publication numbers CCDC 638176 (CCDC, 12 Union Road, Cambridge, CB2 1EZ, UK; e-mail deposit@ccdc.cam.ac.uk).

Acknowledgements

Financial support from the Polish State Committee for Scientific Research, Grant No. 3 T09A 151 27 is kindly acknowledged. Marina S. Fonari thanks the Foundation for Polish Science (FNP) and Mianowski Fund for received grant.

The X-ray measurements were undertaken in the Crystallographic Unit of the Physical Chemistry Laboratory at the Chemistry Department of the University of Warsaw.

Note

1. On leave from the Institute of Applied Physics, Academy of Science, Republic of Moldova, Kishinev, Moldova.

References

- (1) Lehn, J.-M.; Atwood, J.L.; Davies, J.E.D.; McNicol, D.D.; Vögtle, F.; Eds.; *Comprehensive Supramolecular Chemistry*; Pergamon: New York, 1996; Vol. 1.
- (2) Luboch, E.; Bilewicz, R.; Kowalczyk, M.; Wagner-Wysiecka, E.; Biernat, J.F. Azo Macrocyclic Compounds. In *Advances in Supramolecular Chemistry*; Gokel, G.W., Ed.; Cerberus Press: South Miami, 2003; Vol. 9, pp 71–162.
- (3) Skwierawska, A.; Inerowicz, H.; Biernat, J.F. *Tetrahedron Lett.* **1998**, *39*, 3057–3060; Wagner-Wysiecka, E.; Skwierawska, A.; Kravtsov, V.Ch.; Biernat, J.F. *J. Supramol. Chem.* **2001**, *1*, 77–85; Wagner-Wysiecka, E.; Luboch, E.; Marczak, B.; Biernat, J.F. *Pol. J. Chem.* **2001**, *75*, 1457; Inerowicz, H. *J. Incl. Phenom.* **2001**, *39*, 211–214.
- (4) Vögtle, F.; Weber, E. *Angew. Chem., Int. Ed. Engl.* **1979**, *18*, 753–758.
- (5) (a) Wyglądacz, K.; Malinowska, E.; Szczygelska-Tao, J.; Biernat, J.F. *J. Incl. Phenom.* **2001**, *39*, 303–308; (b) Szczygelska-Tao, J.; Biernat, J.F. *Pol. J. Chem.* **2002**, *76*, 931–936.
- (6) Wagner-Wysiecka, E.; Luboch, E.; Kowalczyk, M.; Biernat, J.F. *Tetrahedron* **2003**, *59*, 4415–4420.
- (7) Wagner-Wysiecka, E.; Jamrógiewicz, M.; Luboch, E.; Szczygelska-Tao, J.; Skwierawska, A.; Gwiazda, M.; Klonkowski, A.M.; Biernat, J.F. *Ann. Pol. J. Chem.* **2004**, *3*, 847.
- (8) Goldenberg, L.M.; Biernat, J.F.; Petty, M.C. *Langmuir* **1998**, *14*, 1236–1241.
- (9) Umezawa, Y.; Bühlmann, P.; Umezawa, K.; Thoda, K.; Amemiya, S. *Pure Appl. Chem.* **2000**, *72*, 1851–2082.
- (10) Luboch, E.; Wagner-Wysiecka, E.; Fainerman-Melnikova, M.; Lindoy, L.F.; Biernat, J.F. *Supramol. Chem.* **2006**, *18*, 593–601.
- (11) Wagner-Wysiecka, E.; Jamrógiewicz, M.; Fonari, M.S.; Biernat, J.F. *Tetrahedron* **2007**, *63*, 4414–4421.
- (12) Glenny, M.W.; Lacombe, M.; Love, J.B.; Blake, A.J.; Lindoy, L.F.; Luckay, R.C.; Gloe, K.; Antonioli, B.; Wilson, C.; Schroder, M. *New J. Chem.* **2006**, *30*, 1755–1767.
- (13) Hunter, C.A.; Sanders, J.K.M. *J. Am. Chem. Soc.* **1990**, *112*, 5525–5534.
- (14) Kumar, S.; Bhalla, V.; Singh, H. *Tetrahedron* **1998**, *54*, 5575–5586.
- (15) Luboch, E.; Biernat, J.F.; Muszalska, E.; Bilewicz, R. *Supramol. Chem.* **1995**, *5*, 201–210.
- (16) IUPAC recommendations, *Pure Appl. Chem.* **1970**, *48*, 129.
- (17) Oxford Diffraction 2001; CrysAlis CCD and CrysAlis RED. Oxford Diffraction Poland, Wrocław, Poland.
- (18) Sheldrick, G.M. *Acta Crystallogr.* **1990**, *A46*, 467–473.
- (19) Sheldrick, G.M. SHELXL93. *Program for the Refinement of Crystal Structures*, University of Göttingen, Germany.